LUND UNIVERSITY

Parametrization of the local scattering function estimator for vehicular-to-vehicular channels

Bernadó, Laura; Zemen, Thomas; Paier, Alexander; Kåredal, Johan; Fleury, Bernard

[Link to publication](#)

Parametrization of the Local Scattering Function Estimator for Vehicular-to-Vehicular Channels

Laura Bernadó[1], Thomas Zemen[1], Alexander Paier[2], Johan Karedal[3] and Bernard H. Fleury[1,4]

[1]Forschungszentrum Telekommunikation Wien (ftw.), Vienna, Austria
[2]Institut für Nachrichtentechnik und Hochfrequenztechnik, Technische Universität Wien, Vienna, Austria
[3]Department of Electrical and Information Technology, Lund University, Sweden
[4]Department of Electronics Systems, Aalborg University, Denmark
contact: bernado@ftw.at

Abstract—Non wide-sense stationary (WSS) uncorrelated-scatterering (US) fading processes are observed in vehicular communications. To estimate such a process under additive white Gaussian noise we use the local scattering function (LSF). In this paper we present an optimal parametrization of the multitaper-based LSF estimator. We do this by quantizing the mean square error (MSE). For that purpose we use the structure of a two-dimensional Wiener filter and optimize the parameters of the estimator to obtain the minimum MSE (MMSE). We split the observed fading process in WSS regions and analyze the influence of the estimator parameters on the MMSE under different lengths of the stationarity regions and signal-to-noise ratio values. The analysis is performed considering three different scenarios representing different scattering properties. We show that there is an optimal combination of estimator parameters for different lengths of stationarity region and signal-to-noise ratio values which provides a minimum MMSE.

I. INTRODUCTION

In vehicular communications the fading process does not fulfill the wide-sense stationary (WSS) uncorrelated-scattering (US) property. Methods have been proposed to deal with non-WSSUS processes by repeating the experiment and performing the second-order statistics calculation with the obtained samples instead of in the temporal domain [1]. In reality it is very difficult to obtain different realizations of the same experiment while keeping the same experimental conditions. Therefore, we use the idea of splitting an observed process in small regions, in which we can assume that the WSSUS property holds [2]. In [3] the length of these stationarity regions is assessed by means of the collinearity measure without optimizing the estimator parameters. In [2] an analysis of the estimator parameters is done for pedestrian mobility. In this paper we compute the optimal parametrization of the local scattering function (LSF) estimator for vehicular scenarios. We minimize the mean square error (MSE) taking into account the length of the WSSUS region and different values of signal-to-noise ratio (SNR). We only dispose of the measured finite length channel impulse response and we want to characterize an estimator of the second-order statistics of a process. Since

we do not know the true scattering function of the process, we use a Wiener filter that relates these two measures and allows us to calculate the MSE.

Contributions of the Paper

The objective of the paper is to characterize the properties of the LSF estimator introduced in [2]. The estimator is used to calculate the scattering function of non-stationary processes. In order to assess the performance of the estimator, we define the MSE based on the structure of a two-dimensional (2D) Wiener filter [4]. We show that the Wiener filter coefficients can be calculated from the LSF. We do not use the Wiener filter for filtering a signal, but for characterizing the performance of an estimator. Furthermore, we assess the performance and parameter behavior of the LSF for different vehicular scenarios and SNR values.

Organization of the Paper

In Section II we introduce the 2D Wiener filter concept to calculate the MSE of the estimator. In Section III the relation between the LSF and the filter coefficients is defined. The calculation of the filter coefficients and their optimization, i.e. the choice of the estimator parameters which minimizes the MSE, are analyzed in Sections IV and V respectively. Conclusions are presented in Section VI. Time t, frequency f, delay τ and Doppler shift ν are discrete variables.

II. 2D WIENER FILTER

We want to optimize the parameters of the LSF estimator. In order to do that, we use a 2D time-frequency Wiener filter described in Fig. 1 [4]. We consider a signal $R(t, f)$ to be filtered which consists of the true channel transfer function $H(t, f)$ corrupted with additive complex Gaussian noise $N(t, f)$. The filter coefficients are calculated from the estimated scattering function with the LSF estimator. The optimum LSF parameter set minimizes the MSE between the output of the filter $\hat{H}(t, f)$ and $H(t, f)$.

The estimated transfer function at the filter output reads

$$\hat{H}(t, f) = \sum_{i=0}^{M-1} \sum_{j=0}^{N-1} a_{i,j} R(t-i, f-j) \tag{1}$$

where $a_{i,j}$ are the filter coefficients and M and N denote the length of the sequence $R(t,f)$ in time and frequency respectively. The MSE is given by

$$\mathcal{E} = E\{|e(t,f)|^2\}$$

where $e(t,f) = H(t,f) - \hat{H}(t,f)$ and $E\{\}$ denotes expectation. In order to find the coefficients of this 2D filter, we use the orthogonality principle

$$E\{e(t,f)\hat{H}^*(t'',f'')\} = 0$$

to obtain the Wiener-Hopf equation

$$E\{H(t,f)R^*(t'',f'')\} = \sum_{t',f'} a(t',f',t,f)$$
$$E\{R(t',f')R^*(t'',f'')\}. \quad (2)$$

We assume that the noise $N(t,f)$ is a zero-mean process statistically independent of the channel frequency response $H(t,f)$. Under this assumption we can rewrite (2) as

$$E\{H(t,f)H^*(t'',f'')\} = \sum_{t',f'} a(t',f',t,f)$$
$$E\{R(t',f')R^*(t'',f'')\}. \quad (3)$$

From (3) we see that $E\{H(t,f)H^*(t'',f'')\}$ is the time-frequency (TF) auto-correlation function (ACF) of $H(t,f)$. Similarly, $E\{R(t',f')R^*(t'',f'')\}$ is the TF-ACF of $R(t,f)$. For short we rename these two TF-ACFs as R_H and R_R. In order to define the Wiener filter, we must assume to have stationary processes, therefore the TF-ACFs will depend only on the time and frequency lags and can be expressed as $R_H(\Delta t, \Delta f)$ and $R_R(\Delta t, \Delta f)$.

For the sake of simplicity, we use the compact notation for (3): $\mathbf{R}_H = \mathbf{A}\,\mathbf{R}_R$. From this identity we obtain the coefficients of the 2D Wiener filter:

$$\mathbf{A^T} = \mathbf{R}_H^T \mathbf{R}_R^{-1} \quad (4)$$

with

$$\mathbf{R}_R = \begin{bmatrix} \mathbf{R}_R(\Delta t, 0) & \cdots & \mathbf{R}_R(\Delta t, N-1) \\ \vdots & \ddots & \vdots \\ \mathbf{R}_R^H(\Delta t, N-1) & \cdots & \mathbf{R}_R(\Delta t, 0) \end{bmatrix},$$

where

$$\mathbf{R}_R(\Delta t, 0) = \begin{bmatrix} R_R(0,0) & \cdots & R_R(M-1,0) \\ \vdots & \ddots & \vdots \\ R_R^*(M-1,0) & \cdots & R_R(0,0) \end{bmatrix}.$$

In the above expressions, $()^H$ denotes Hermitian transposition and $()^*$ complex conjugation. The matrix $\mathbf{R}_H$ follows the same structure, whereas $\mathbf{A}$ stems from rewriting (1) in matrix notation, i.e. $\hat{\mathbf{h}} = \mathbf{A^T r}$, where the vectors $\hat{\mathbf{h}}$ and $\mathbf{r}$ are the channel transfer function and its noisy version respectively. They are similarly defined as

$$\hat{\mathbf{h}} = \begin{bmatrix} \underline{\hat{h}}^T(0) \\ \vdots \\ \underline{\hat{h}}^T(M-1) \end{bmatrix} \quad \text{with} \quad \underline{\hat{h}}(0) = \begin{bmatrix} \hat{H}(0,0) \\ \vdots \\ \hat{H}(0,N-1) \end{bmatrix}.$$
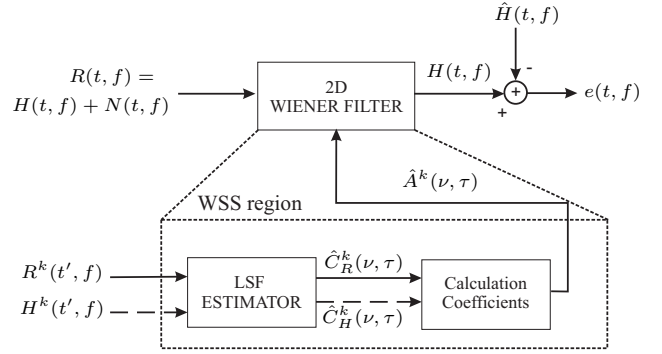

Fig. 1. Calculation of the filter coefficients for each *WSS* region.

III. FILTER IMPLEMENTATION

The TF filter in (1) can be written as the 2D TF-convolution

$$\hat{H}(t,f) = a(t,f) * R(t,f) \quad (5)$$

with $a(t,f)$ denoting the filter coefficients defined in (4). Performing the Fourier transform in both dimensions, we can express (5) as

$$\mathcal{F}_t\mathcal{F}_f^{-1}\left\{\hat{H}(t,f)\right\} = \mathcal{F}_t\mathcal{F}_f^{-1}\{a(t,f) * R(t,f)\} \quad (6)$$
$$S_{\hat{H}}(\nu,\tau) = A(\nu,\tau)S_R(\nu,\tau),$$

where $S_{\hat{H}}(\nu,\tau)$ and $S_R(\nu,\tau)$ are the Doppler-delay spreading functions of $\hat{H}(t,f)$ and $R(t,f)$. In (6) $\mathcal{F}$ and $\mathcal{F}^{-1}$ denote the Fourier transform and its inverse respectively. The filter coefficients $A(\nu,\tau)$ in (4) are given by

$$A(\nu,\tau) = \mathcal{F}_t\mathcal{F}_f^{-1}\left\{\frac{R_H(\Delta t, \Delta f)}{R_R(\Delta t, \Delta f)}\right\}$$
$$= \frac{|S_H(\nu,\tau)|^2}{|S_R(\nu,\tau)|^2} = \frac{C_H(\nu,\tau)}{C_R(\nu,\tau)} \quad (7)$$

with $C_H(\nu,\tau)$ and $C_R(\nu,\tau)$ denoting the Doppler-delay scattering functions of $H(t,f)$ and $R(t,f)$ respectively. Since we know the true channel transfer function we are able to calculate $S_H(t,f)$ and $C_H(t,f)$ directly from $H(t,f)$. In order to obtain $\hat{H}(t,f)$ we only need to reverse the sequence of Fourier transforms performed in (6) at the output of the filter.

IV. CALCULATION OF THE FILTER COEFFICIENTS

The filter coefficients determined in (7) depend on the scattering functions $C_R(\nu,\tau)$ and $C_H(\nu,\tau)$. We calculate an estimate of them using a multitaper estimator in which the windows are chosen to be the discrete prolate spheroidal sequences (DPSS) [5]. Since we are dealing with non-WSS processes, the observed process at the input of the filter is divided in time regions over which we can assume that the WSS property holds. The WSS region is finite with dimensions M in time and N in frequency. This allows us to calculate the second-order moments of the process and, consequently, the filter coefficients. Since everything takes place locally, the estimate of the scattering function in (8)

is named local scattering function (LSF) [2], [6]. The filter coefficients defined in (7) will be also local. They are fed back to the filter after the estimation procedure (Fig. 1). In order to show explicitly this locality, we introduce the superscript k in the notation. The time variables t, t', and k are related through $t = Mk + t'$ where $k = 0 \ldots \lfloor S/M \rfloor - 1$ and $t' = 0 \ldots M - 1$. The sampled version of the LSF estimate $\hat{C}_H(\nu, \tau)$ [7] reads

$$\hat{C}_H^k(\nu, \tau) = \frac{1}{IJ} \sum_{l=0}^{L-1} \left| \mathcal{H}^{k\,(G_l)}(\nu, \tau) \right|^2. \qquad (8)$$

The ranges of the variables τ and ν in (8) are $\{0, \ldots, N-1\}$ and $\{-M/2, \ldots M/2 - 1\}$ respectively. The number of tapers in time and frequency are I and J respectively and

$$\mathcal{H}^{k\,(G_l)}(\nu, \tau) = \sum_{t''=-M/2}^{M/2-1} \sum_{f''=-N/2}^{N/2-1} H(t'' - t, f'')$$
$$G_l(t'', f'') e^{-j2\pi(\nu t'' - \tau f'')} \qquad (9)$$

is the tapered version of $H(t, f)$ and $G_l(t'', f'') e^{-j2\pi(\nu t'' - \tau f'')}$ are the DPSS time-frequency tapers. The filter coefficients are calculated from estimated functions, therefore we will use estimates of the filter coefficients, $\hat{A}^k(\nu, \tau)$. The local filter coefficients are defined as

Even though this solution is considered optimal for the Wiener-filtering problem, our estimation of the LSF forces us to perform another optimization step. In the estimator (8) there is an optimal number of windows in time and frequency that reduces the overall MSE.

V. OPTIMIZATION OF THE PARAMETERS OF THE ESTIMATOR

Recent measurements have reported non-stationary channel responses for vehicle-to-vehicle propagation [8], and we therefore make use of such measurements to demonstrate a solution for the above optimization problem. Further details regarding the measurements are found in [8]. As observed in [7], communications between vehicle with opposite driving directions experience the largest temporal variations. We consider three such scenarios (transmitter and receiver move at the same speed):

Scenario 1 (S1): Highway environment. There is a strong line of sight (LOS) component with diffuse components and some reflecting paths. Considered speeds: (*a*) 110 km/h and (*b*) 90 km/h.

Scenario 2 (S2): Rural environment. There is a strong LOS component with diffuse components but no additional paths. Considered speeds: (*a*) 70 km/h and (*b*) 50 km/h.

Scenario 3 (S3): Urban environment. There is a strong LOS component with large diffuse contributions and additional paths created by reflections coming from near objects. Considered speeds: (*a*) 50 km/h and (*b*) 30 km/h.

In scenario 1 (highway) the delay spread is short and some contributions arrive at late delays. In scenario 2 (rural) the delay spread is longer with no further contributions. In scenario 3 (urban) the largest delay spread is observed with lots

(a) *S1-a* (Highway-110 km/h) (b) *S1-b* (Highway-90 km/h)

(c) *S2-a* (Rural-70 km/h) (d) *S2-b* (Rural-50 km/h)

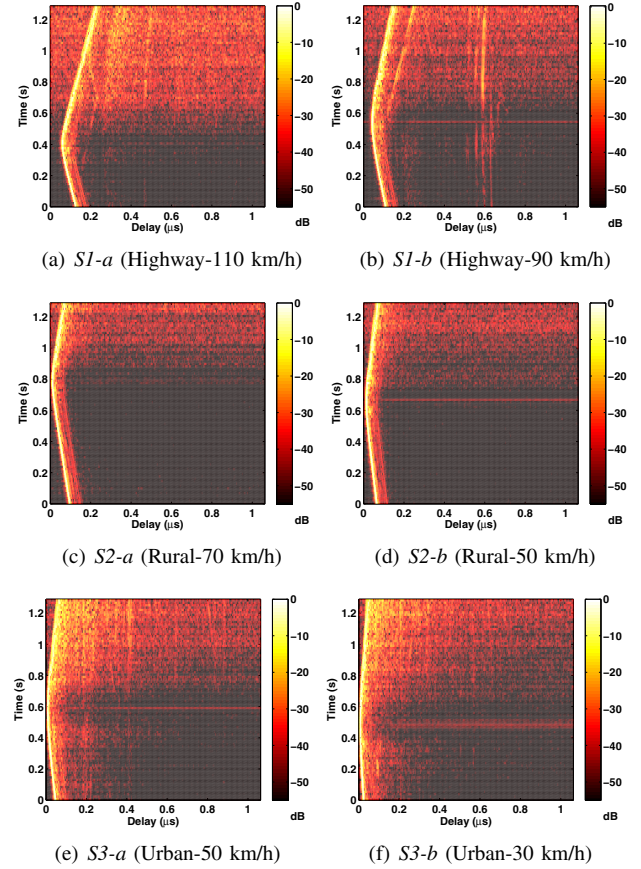(e) *S3-a* (Urban-50 km/h) (f) *S3-b* (Urban-30 km/h)

Fig. 2. Normalized squared envelope of the channel response measured in the three investigated scenarios.

of paths coming from close reflecting objects. Figure 2 shows the squared magnitude of the time-varying impulse responses measured in the three scenarios. Since the measured channel transfer functions have a SNR of roughly 40 dB, we consider these as the true transfer functions $H(t, f)$. Noise-corrupted transfer functions $R(t, f)$ are created by adding random complex Gaussian noise to $H(t, f)$. Since in all scenarios we are in LOS situation, the measured channel impulse response is very peaky. If we consider a very bad situation, when the signal is quasi completely covered by noise, we have to evaluate a SNR of -15 dB. We also analyze in this section the impact of different SNR values in the estimator parameters. Figure 3 shows the noise-corrupted channel impulse response for different SNR values.

We use the sampled channel transfer function $H(t, f) = H(t_{\text{cont}} T_{\text{rep}}, f_{\text{cont}} B/Q)$, where $T_{\text{rep}} = 307.2 \mu s$ is the repetition time of the channel sounder, $B = 240$ MHz is the measurement bandwidth and $Q = 256$ is the number of frequency bins. The variables t_{cont} and f_{cont} are continuous. We consider a measurement run of 1.32 s with $f \in \{0 \ldots Q - 1\}$ and $t \in \{0 \ldots S - 1\}$, where $S = 4322$ samples.

A. Number of Time-Frequency Tapers (Choice of (I, J)):

In a first step we select a given stationarity length M and optimize the parameters I and J. For this first analysis we set $M = 64$ and SNR= -15 dB. The choice of the time-

TABLE I
MMSE AND OPTIMAL (I, J) COMBINATION FOR DIFFERENT SCENARIOS, DIFFERENT WSS REGION LENGTHS, AND SNR VALUES.

sce-nario	SNR (dB)	WSS region length M				sce-nario	SNR (dB)	WSS region length M			
		64	128	256	512			64	128	256	512
S1-a	-15	-7.37 (1,4)	-7.78 (3,3)	-8.16 (3,3)	-7.84 (5,3)	S1-b	-15	-8.73 (1,4)	-9.24 (3,3)	-9.75 (3,3)	-9.31 (3,3)
	-5	-10.19 (1,5)	-10.52 (3,4)	-10.99 (3,4)	-10.92 (3,4)		-5	-12.59 (3,3)	-13.07 (3,4)	-13.87 (3,4)	-13.79 (3,4)
	5	-13.41 (1,5)	-13.56 (3,4)	-13.95 (3,4)	-13.95 (3,4)		5	-16.54 (3,4)	-16.84 (3,4)	-17.62 (3,4)	-17.64 (3,4)
	15	-18.96 (3,4)	-18.99 (3,4)	-19.21 (3,4)	-19.24 (3,4)		15	-21.37 (3,4)	-21.49 (3,4)	-22.08 (3,4)	-22.08 (3,4)
S2-a	-15	-9.89 (1,4)	-10.41 (3,3)	-11.26 (3,3)	-11.20 (5,3)	S2-b	-15	-9.98 (1,4)	-10.78 (3,3)	-11.45 (3,3)	-11.28 (5,3)
	-5	-14.19 (1,3)	-14.58 (3,4)	-15.74 (3,4)	-16.05 (3,4)		-5	-14.41 (3,3)	-15.00 (3,4)	-15.80 (3,3)	-15.88 (5,4)
	5	-18.48 (3,4)	-18.70 (3,4)	-20.00 (3,4)	-20.31 (3,4)		5	-18.83 (3,4)	-19.17 (3,4)	-19.83 (3,4)	-19.87 (3,4)
	15	-23.28 (3,4)	-23.47 (3,4)	-24.32 (3,4)	-24.68 (3,4)		15	-23.37 (3,4)	-23.47 (3,4)	-23.98 (3,4)	-23.98 (3,4)
S3-a	-15	-7.66 (1,4)	-8.29 (3,3)	-8.96 (3,3)	-9.11 (3,3)	S3-b	-15	-8.30 (1,4)	-9.50 (3,3)	-9.96 (3,3)	-10.25 (3,4)
	-5	-11.89 (1,4)	-12.47 (3,4)	-13.10 (3,4)	-13.44 (3,4)		-5	-12.43 (1,4)	-13.24 (3,4)	-14.11 (3,4)	-14.51 (3,4)
	5	-16.63 (3,4)	-17.05 (3,4)	-17.62 (3,4)	-17.96 (3,4)		5	-17.12 (1,5)	-17.72 (3,4)	-18.45 (3,4)	-18.80 (3,4)
	15	-21.87 (3,4)	-22.08 (3,4)	-22.52 (3,4)	-22.76 (3,4)		15	-22.29 (3,4)	-22.68 (3,4)	-23.28 (3,4)	-23.47 (3,4)

bandwidth product determines the number of tapers used in the estimation process [9]: $I < 2N_tW_t$ in the time domain and $J < 2N_fW_f$ in the frequency domain, where $N_tW_t = i/\Delta t$ and $N_fW_f = j/\Delta\tau$ ($N_tW_t = i$ and $N_fW_f = j$ when using normalized Δt and $\Delta\tau$). Our optimization problem is thus to solve

$$\underset{I,J}{\arg\min} \left(\frac{1}{K} \sum_k \mathcal{E}^k \right).$$

The term to be optimized is the mean of the MSE per region, computed over a total number of K WSS regions. The normalized MSE per region is defined as

$$\mathcal{E}^k = \frac{\sum_{t'=1}^{M} \sum_{f=1}^{N} |H^k(Mk+t', f) - \hat{H}^k(Mk+t', f)|^2}{\sum_{t'=1}^{M} \sum_{f=1}^{N} |H^k(Mk+t', f)|^2}$$

with $I < 2i$, $J < 2j$, and M, N denoting the extent of the WSS region. We evaluate the MSE for all possible combinations of I and J from 1 to 6. Figure 4 plots the obtained MSEs using the gray-scale code reported on the right for different (I, J) pairs for scenario S1-a. We highlight the minimum MSE with a red square at the pair (I, J) which achieves it.

While increasing the number of tapers in both time and frequency domains the MSE decreases rapidly and beyond a certain point starts to grow slowly. This is due to the fact that, by increasing the number of tapers, on one hand we reduce the variance, but on the other hand we increase the bias. There is a trade-off between these two effects which
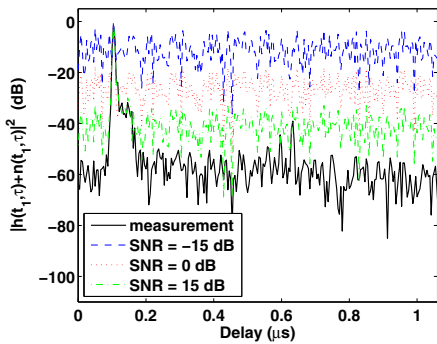

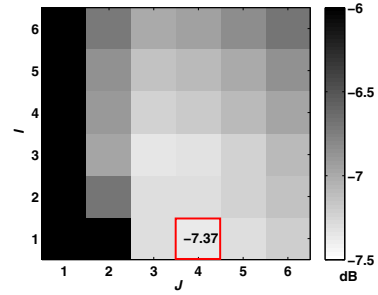Fig. 3. Snapshot of a channel impulse response with additive Gaussian noise for different SNRs values.

Fig. 4. MSE versus (I, J) for S1-a. SNR=−15dB and $M = 64$.

corresponds to the best combination of the number of tapers in time and frequency to minimize the MSE. A similar behavior is observed for all tested scenarios.

B. Length of the Stationarity Region:

The stationarity region is defined by two parameters: M (for the time domain) and N (for the frequency domain). M has to be selected in order to ensure the WSS property and N the US property. When choosing M properly, we can also ensure that contributions at different delays are not correlated (they come from different scatterers). The length of this region should be short enough to ensure the US property to hold within one WSS region. We define different regions with lengths $M = 64, 128, 256$, and 512 samples and calculate the MSE.

Although the optimization of the number of tapers was done previously in Sec. V-A, here we analyze the dependency of the length of the stationarity region with the optimal (I, J) pair. Table I reports the results plotted in Fig. 5.

The MMSE depends on M. When we increase the length of the WSS region, we observe a longer period of time and consequently more variations of the process. Thus, we need to consider more windows in our multitaper estimator (Tab. I).

In Fig. 5, for a given scenario (we compare curves with the same color/marker), the achieved MMSE is smaller for the case (b), i.e. when the cars drive slower. The less time-varying the channel is (the slower the cars drive), the smaller the achieved MMSE is. This tendency is kept for different SNRs.

Due to the speed of the cars it is clear that there are more time fluctuations in scenario 1 and results in the largest
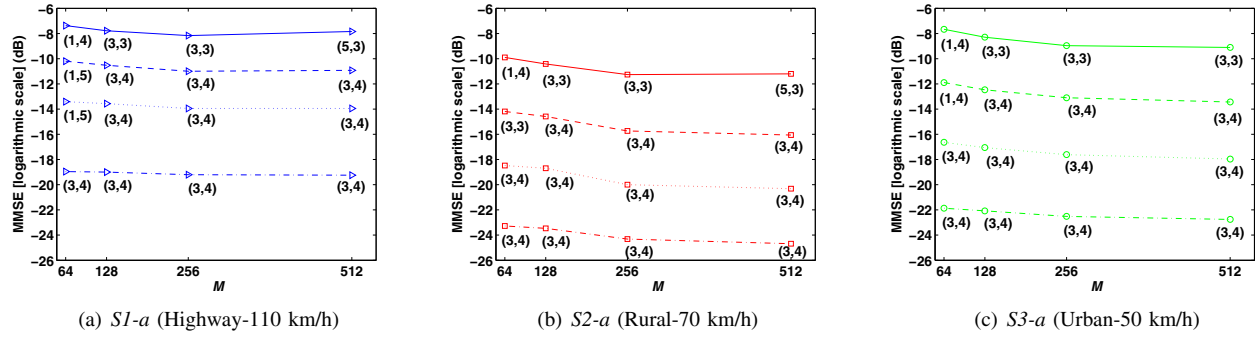
(a) *S1-a* (Highway-110 km/h) (b) *S2-a* (Rural-70 km/h) (c) *S3-a* (Urban-50 km/h)

Fig. 6. Influence of SNR in the MMSE for different scenarios. SNR$= -15$ dB (solid line), SNR$= -5$ dB (dashed line), SNR$= 5$ dB (dotted line), SNR$= 15$ dB (dash-dotted line).

MMSE. Even though the cars in scenario 3 drive slower than in scenario 2, scenario 3 presents a larger MMSE. This is due to the large delay spread and numerous path contributions in scenario 3 where we observe a more unstationary process.

C. Signal-to-Noise Ratio Values:

So far the presented results have been calculated with a SNR of -15 and 5 dB. Table I shows the results for different SNR values plotted in Fig. 6, only for scenario versions *a*. When increasing the SNR, the multipath contributions become more visible in the noise corrupted channel transfer function, and therefore we need more tapers to well represent them. The achieved MMSE decreases as SNR increases.

The influence of the choice of M is strong only for very bad SNR conditions. We observe a continuous decrease of the MMSE for high SNR values also for long WSS regions. Even though the MMSE continues decreasing with increasing M for high SNRs, we should be careful in extending the length of the stationarity region, due to the violation of the US assumption, and consequently we would not be allowed to calculate the second-order moments of the process.

VI. CONCLUSIONS

We assessed the performance of the local scattering function (LSF) by means of the mean square error (MSE). For that purpose we used a two-dimensional Wiener filter. We showed that there is a best parameters combination for the LSF which results in the minimum MSE (MMSE) and that the MSE decreases until it reaches a minimum and increases again

when the number of tapers in the LSF increases. The number of tapers achieving the MMSE increases when considering higher signal-to-noise ratio values. We chose the vehicular communications environment to quantify it. For a given scenario, the slower the cars drive, the smaller the MMSE is. The MMSE depends on the non-stationarity of the environment, being smaller for more stationary scenarios. Due to the high speeds of the cars, the highway scenario is the most time-varying and therefore presents the largest MMSE. The rural scenario presents a short delay spread and no further multipath contributions, thus achieving a small MMSE. Although the speeds of the cars in the urban scenario are the lowest, the scattering environment contributes to creating a long delay spread and therefore a more time-varying environment.

REFERENCES

[1] J. S. Bendat and A. G. Piersol, *Engineering Applications of Correlation and Spectral Analysis*. John Wiley & Sons, Inc, 1963.

[2] G. Matz, "Doubly underspread non-WSSUS channels: Analysis and estimation of channel statistics," in *Proc. IEEE Int. Workshop on Signal Processing Advance Wireless Communications (SPAWC)*, Rome, Italy, June 2003, pp. 190–194.

[3] A. Paier, T. Zemen, L. Bernadó, G. Matz, J. Karedal, N. Czink, C. Dumard, F. Tufvesson, A. F. Molisch, and C. F. Mecklenbräuker, "Non-WSSUS vehicular channel characterization in highway and urban scenarios at 5.2 GHz using the local scattering function," in *Workshop on Smart Antennas (WSA)*, Darmstadt, Germany, February 2008.

[4] S. Kaiser, "Multi-carrier CDMA mobile radio systems-analysis and optimization of detection, decoding and channel estimation," Ph.D. dissertation, German Aerospace Center (DLR). Institute of Communications and Navigation, Germany, 1998.

[5] D. Slepian, "Prolate spheroidal wave functions, Fourier analysis, and uncertainty - V: The discrete case," *The Bell System Technical Journal*, vol. 57, no. 5, pp. 1371–1430, May-June 1978.

[6] G. Matz, "On non-WSSUS wireless fading channels," *IEEE Trans. Wireless Commun.*, vol. 4, no. 5, pp. 2465–2478, September 2005.

[7] L. Bernadó, T. Zemen, A. Paier, G. Matz, J. Karedal, N. Czink, C. Dumard, F. Tufvesson, M. Hagenauer, A. F. Molisch, and C. F. Mecklenbräuker, "Non-WSSUS vehicular channel characterization at 5.2 GHz - spectral divergence and time-variant coherence parameters," in *Proceedings of the XXIXth URSI General Assembly*, Chicago, USA, August 2008.

[8] A. Paier, J. Karedal, N. Czink, H. Hofstetter, C. Dumard, T. Zemen, F. Tufvesson, C. F. Mecklenbräuker, and A. F. Molisch, "First results from car-to-car and car-to-infrastructure radio channel measurements at 5.2 GHz," in *International Symposium on Personal, Indoor and Mobile Radio Communications (PIMRC 2007)*, September 2007, pp. 1–5.

[9] D. B. Percival and A. T. Walden, *Spectral Analysis for Physical Applications*. Cambridge University Press, 1963.
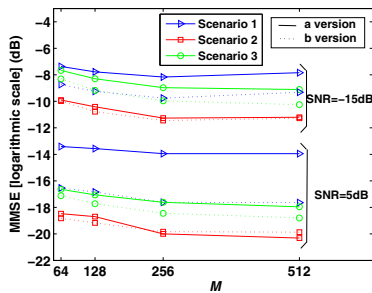
Fig. 5. MMSE versus the WSS-region length for all scenarios and different SNRs.